*GEOLOGICA CARPATHICA, 50, 1, BRATISLAVA, FEBRUARY 1999*
*49–61*

# ORIGIN OF RHYTHMICALLY BEDDED CENOMANIAN CARBONATE ROCKS OF THE BAKHCHISARAI REGION (SW CRIMEA)

IUGS UNESCO IGCP
Project No. 362

RUSLAN GABDULLIN[1], ANDREY GUZHIKOV[2] and IVAN DUNDIN[3]

[1]Moscow State University, Geological Faculty, Department of Historical and Regional Geology, Vorobiovy Gory, 119899 Moscow, Russia; ruslan@geol.msu.su
[2]Geological Institute of Saratov University, Moskovskaya 161, 410750 Saratov, Russia
[3]Saratov State University, Geological Faculty, Department of Geophysics, Astrahanskaya 83, 410071 Saratov, Russia

*(Manuscript received January 14, 1998; accepted in revised form December 11, 1998)*

**Abstract:** Rhythmically bedded marls and limestones were studied in the Cenomanian deposits of SW part of Mountain Crimea in Ukraine. Carbonate content, TOC, XRD, foraminiferal, petromagnetic analyses and ichnofossil distribution analysis were carried out on 115 samples from 6 sections to define the nature of 5 types of rhythmicity. Marl-sandy marl rhythms of the Lower Cenomanian transform into limestone-marl rhythms of the Middle Cenomanian. Upper Cenomanian rocks contain limestone-limestone, limestone-marl rhythms and rhythmically bedded black shales (analog of “Bonarelli level”). The types of the rhythms can be classified due to lithology and their paleogeographic position. Cycles of dilution, solution and bioproduction are involved, 11 paleogeographic models are discussed, 6 are proposed. The nature of the rhythms can be connected with Milankovich cycles.

**Key words:** Crimea, Cenomanian, rhythmicity, carbonate rocks, paleogeographic models.

## Introduction

This study focusses on the depositional history of Cenomanian rhythmically bedded carbonate rocks outcropping in Crimea.

The most important biostratigraphical investigations in the studied region were made by D.P. Naidin and A.S. Alekseev (Naidin & Maslakova 1958; Naidin et al. 1975, 1980; Naidin & Kyashko 1994). Now it is known that Cenomanian deposits have erosional contacts both with the Upper Albian (Mortoniceras inflatum, Stoliczkaia dispar zones) and the Lower Turonian (Whiteinella archeocretacea, Helvetoglobotruncana helvetica zones). The Lower-Middle Cenomanian boundary is erosional too. The thickness of the whole Cenomanian varies from 20 to 70 meters.

Anoxic events are commonly observed near the Cenomanian-Turonian boundary of this region. An example is a “black shale” in the Aksu-Dere section, located in the studied area. This anoxic event was studied in detail by many scientists (Naidin & Kyashko 1994; Gavrilov & Kopaevich 1996; Alekseev et al. 1997).

The Early Cenomanian was a time when a rapid transgression took place. The depth of the basin constantly increased during the Cenomanian up to 500 meters (according to foraminiferal data, Dolitskaya 1972). During the Cenomanian the development of the basin took place under stable tectonic conditions. It must be noted that the paleogeography of this region is poorly investigated. Authors propose paleogeographic sketches for the Lower, Middle and Upper Cenomanian.

The rhythmicity in the part of the Middle Cenomanian was studied by V.T. Frolov (Frolov 1996). Cretaceous rhythmically bedded rocks and paleogeographical models of their origin were investigated by R.R. Gabdullin (Gabdullin 1997; Gabdullin & Baraboshkin 1997).

The following rhythms were observed: (1) Lower Cenomanian: marl-sandy marl (Mantelliceras mantelli Zone, Inoceramus crippsi Subzone), (2) Middle Cenomanian: marl, marly limestone-limestone (Rotalipora cushmani Zone) and (3) Upper Cenomanian: limestone-limestone and limestone-marl, including rhythms in “black shale” (Rotalipora cushmani Zone, Whiteinella archeocretacea Zone).

Cenomanian deposits on the Russian craton are usually presented by mostly terrestrial (sands, sandstones) and rare carbonate rocks. These deposits of variable thickness (0–70 m) with extremely rare rhythmical bedding contain many erosive surfaces and phosphate concretions. That is why we decided to investigate the comparatively «complete» Cenomanian sections of Crimea.

## Methods of study

In the field the succession was divided into rhythms based on the weathering profile (mostly Middle Cenomanian), colour difference and ichnofossil distribution (mostly Middle Cenomanian), thickness variation (exept Late Cenomanian) and distribution of pyrite concretions.

Thin sections of 50 samples were studied. X-ray diffraction analysis (2 samples), foraminiferal analysis (4 samples), total organic carbon content and calcium carbonate content analysis (50 samples) were used. Petromagnetic investigations (115 samples) included measurements of magnetic susceptibility (k), natural remanent magnetization (Jr), remanent saturation magnetization (Jrs), destructive field of remanent saturation magnetization (H'cs) and magnetic susceptibility increase (dk). To determine mineral species with magnetic properties, differential thermal magnetic analysis (DTMA) was used, and JR-4 and IMB-2 machines were used for remanent magnetization and magnetic susceptibility analyses. The studied rocks are characterized by extremely low size of natural magnetization, which is close to the limits of error of the method: magnetic susceptibility varies from $1\times10^{-5}$ to $2\times10^{-5}$ SI (standard units) and natural remanent magnetization changes from 0.005 to 0.05 nT (T=N/Am). The strenght of magnetic susceptibility and natural remanent magnetization increase under the influence of laboratory magnetic field and temperature (k from 5.9 up to 29.3 nT and Jr from 0 to $55\times10^{-5}$). Increasing magnetic susceptibility is connected with the thermal transformation of iron sulphides into magnetite. So the presence of pyrite and pyrrothine in rocks is proved by magnetic susceptibility increase. Vertical graphs of measured parameters do not show cyclic changes but the calculated sizes of Jrs-Hcs correlation, variances of Jrs and H'cs have rhythmic fluctuations (window size — 5 samples, step size — 1 sample). The use of petromagnetic methods can help scientists to: (1) determine low concentrations of sulphide and non-sulphide Fe-magnetics of dust size invisible even in thin sections; (2) to distinguish the composition and volume of the terrestrial input; to understand the nature of magnetic minerals. Petromagnetic methods are good for subdivision and correlation of studied sections. Cyclic distribution of magnetic minerals detected by these methods can be interpreted as cy-

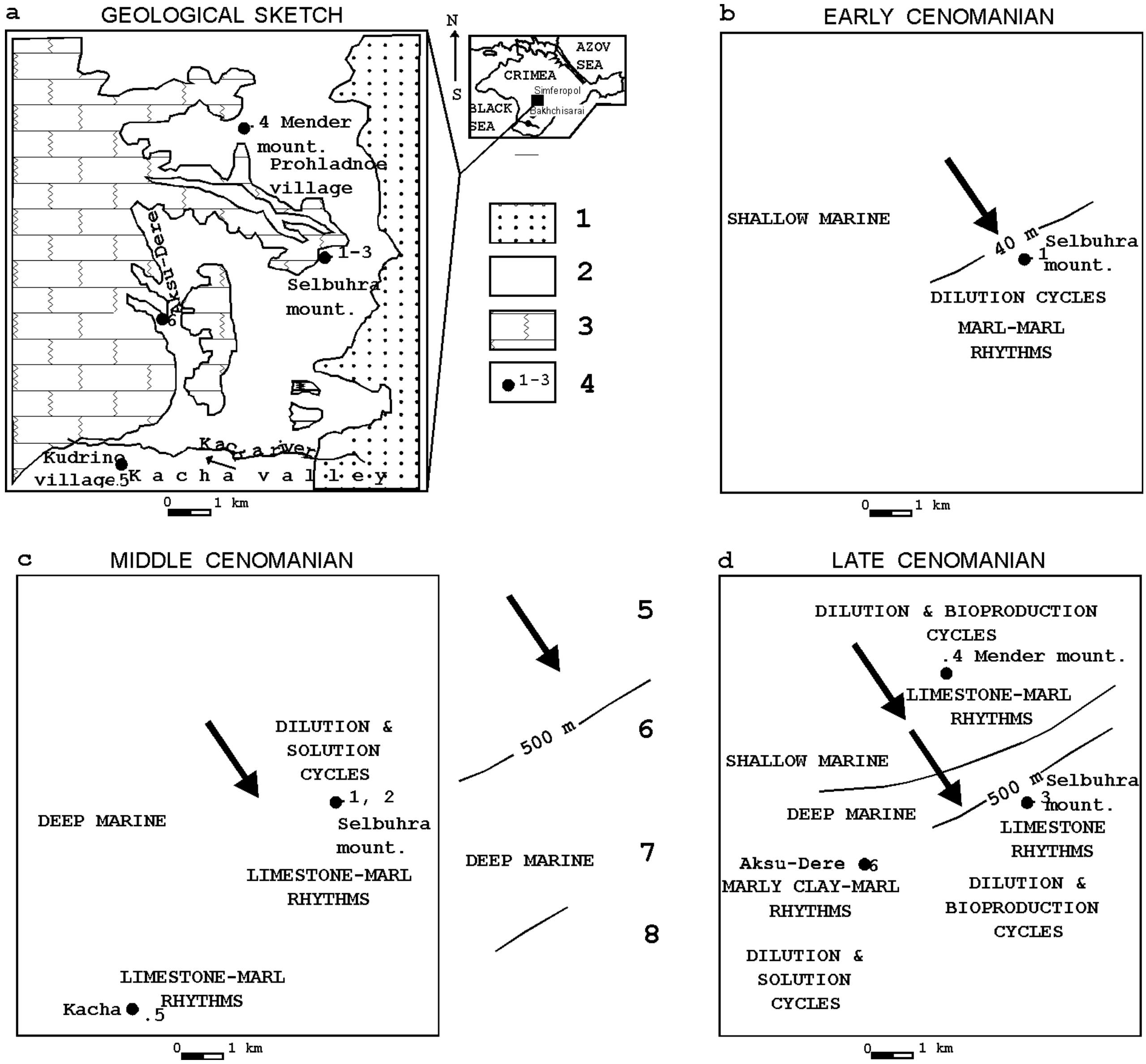


**Fig. 1.** Geological sketch (a) and paleogeographical sketches (b–d) of Bakhchisarai region (SW Crimea) with studied outcrops. Legend: 1 — underlaying rocks; 2 — Cenomanian rocks; 3 — overlaying rocks; 4 — sections (location and number); 5 — direction of the terrestrial input; 6 — depth of the basin (m); 7 — regime, conditions; 8 — proposed boundaries between paleogeographic areas.

cles of dilution (allochthonous Fe-magnetic minerals) or solution (authigenic sulphide Fe-magnetic minerals).

The Kacha section (section 5) was not investigated with the laboratory methods. We used this section for paleogeografical reconstructions.

## Setting

The outcrops are located in the Mountain part of the Crimea Peninsula in the Bakhchisarai region (Figs. 1, 2), include Selbuhra Mts. sections 1–3 (Cenomanian, Figs. 2–4), Kacha Valley, section 5 (probably, Middle Cenomanian, Figs. 2, 3), Mender Mountain, section 4 (Upper Cenomanian, Figs. 2, 6). Section 4 is situated 3 km to the NW from the sections 1–3, which are 7 km to the NE from the section 5. Sections are mostly presented by the alteration of grey and white marls and white marly limestones to limestones. The thickness of limestones is first decimeters, sometimes meters. Marls are centimeters, sometimes meters thick. Section 6 (Aksu-Dere Valley, Figs. 2, 7) is represented by Upper Cenomanian–Lower Turonian (Rotalipora cushmani, Whiteinella archeocretacea zones) rhythmically bedded marls and marly clays inside "black shale". Aksu-Dere section is located about 4.5 km to the SE from Selbuhra sections (1–3).

Section 1. Lower Cenomanian part of the section consists of 7 rhythms, with a visible thickness is of 6.7 m. The Middle Cenomanian part of the section consists of 29 rhythms, 59 beds, their visible thickness is 13.1 m (Fig. 2). Section 2. The

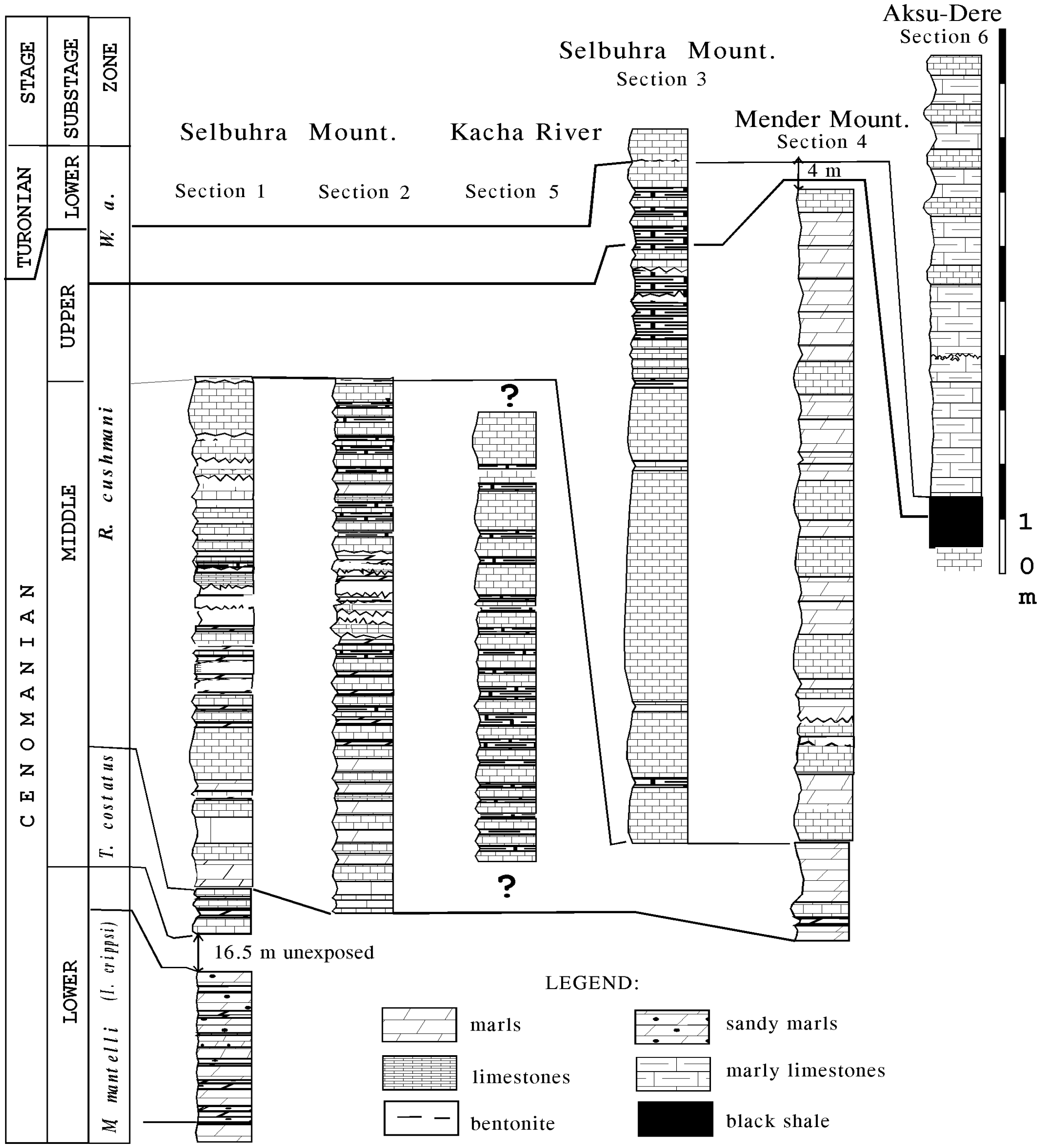


**Fig. 2.** Correlation scheme of Cenomanian rocks of the Bakhchisarai region (SW Crimea).

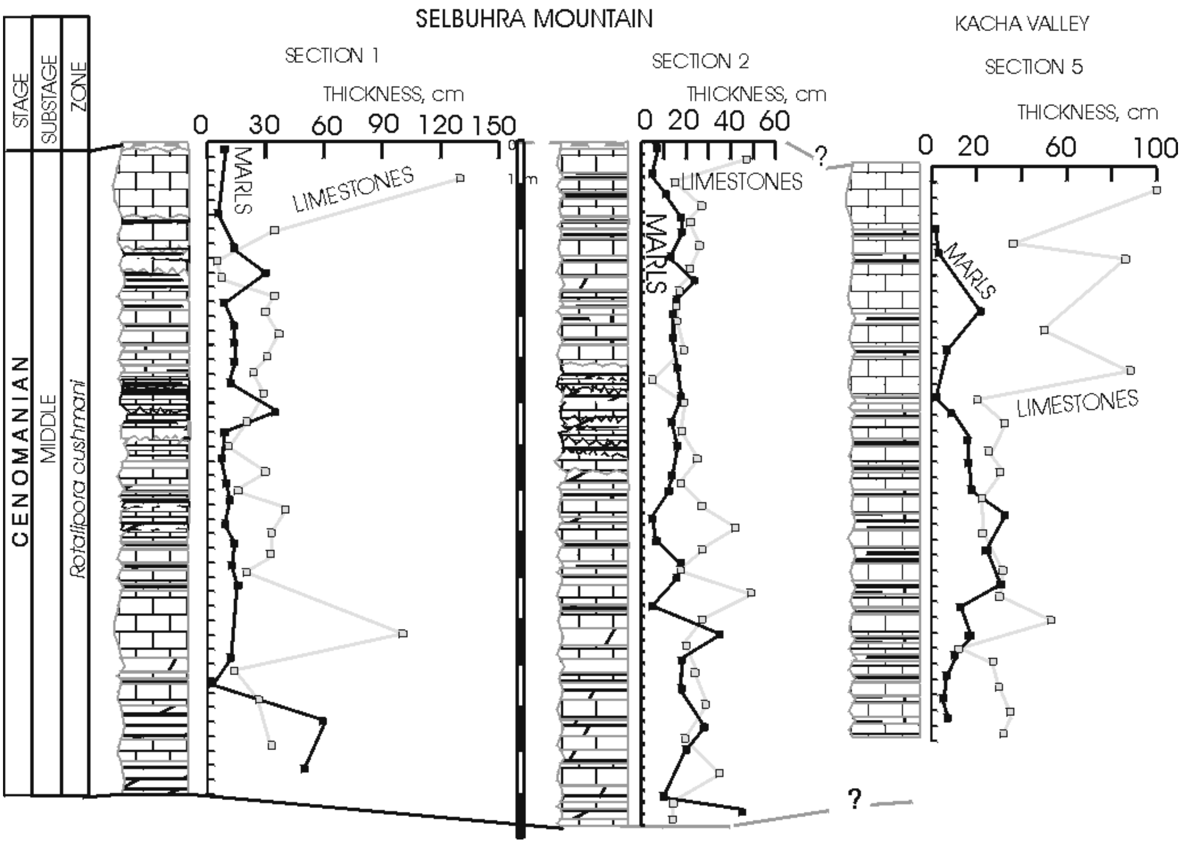


**Fig. 3.** Scheme of correlation and beddings thickness distribution of Middle Cenomanian rocks, Bakhchisarai region, SW Crimea.

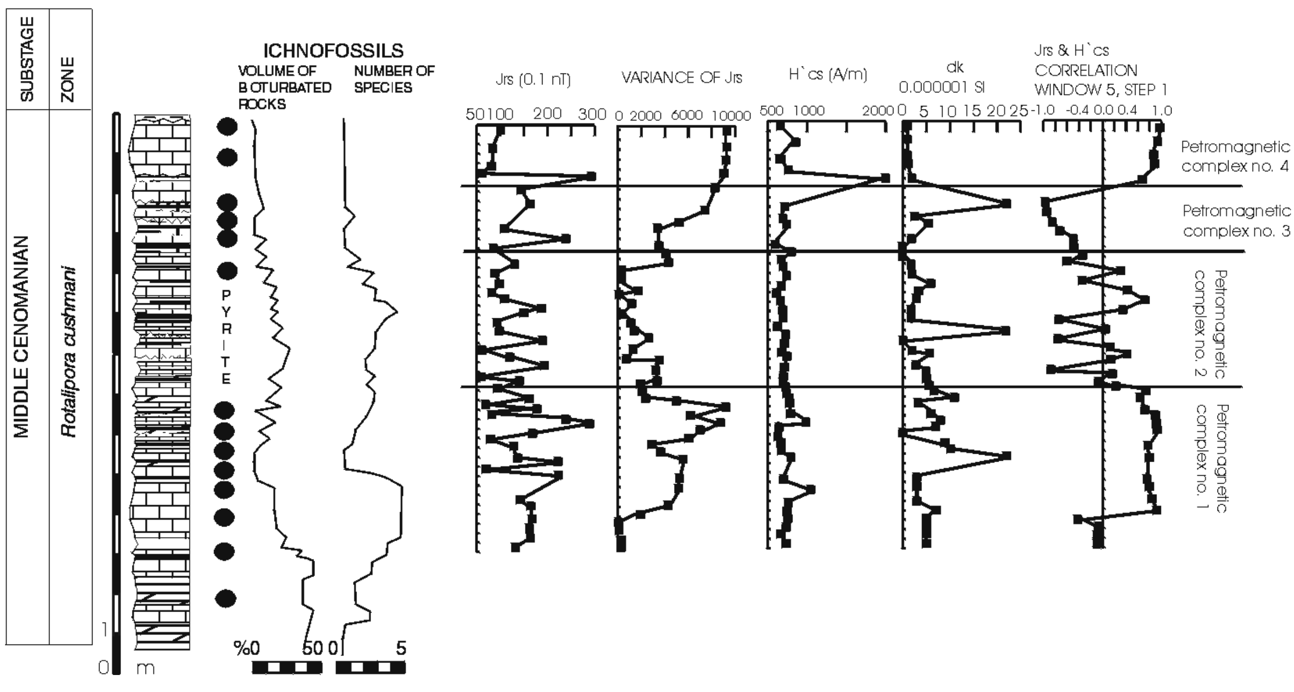


**Fig. 4.** The variation of ichnofossils and petromagnetic parameters in Middle Cenomanian of Selbuhra Mountain, SW Crimea.

Middle Cenomanian consists of 22 rhythms, 45 beds, their visible thickness is 12.4 m (Figs. 3–5). Section 3. The Upper Cenomanian consists from 9 rhythms, 19 beds, thickness is 12.1 m (Fig. 4). Section 4. The Upper Cenomanian consists of 9 rhythms, 19 beds, their thickness is 12 m (Fig. 6). Section 5. The Middle Cenomanian consists of 9 rhythms, 18 beds, their visible thickness is 11 m (Fig. 3). Section 6 include 15 layers, 6 rhythms, thickness is 1.5 m (Fig. 7).

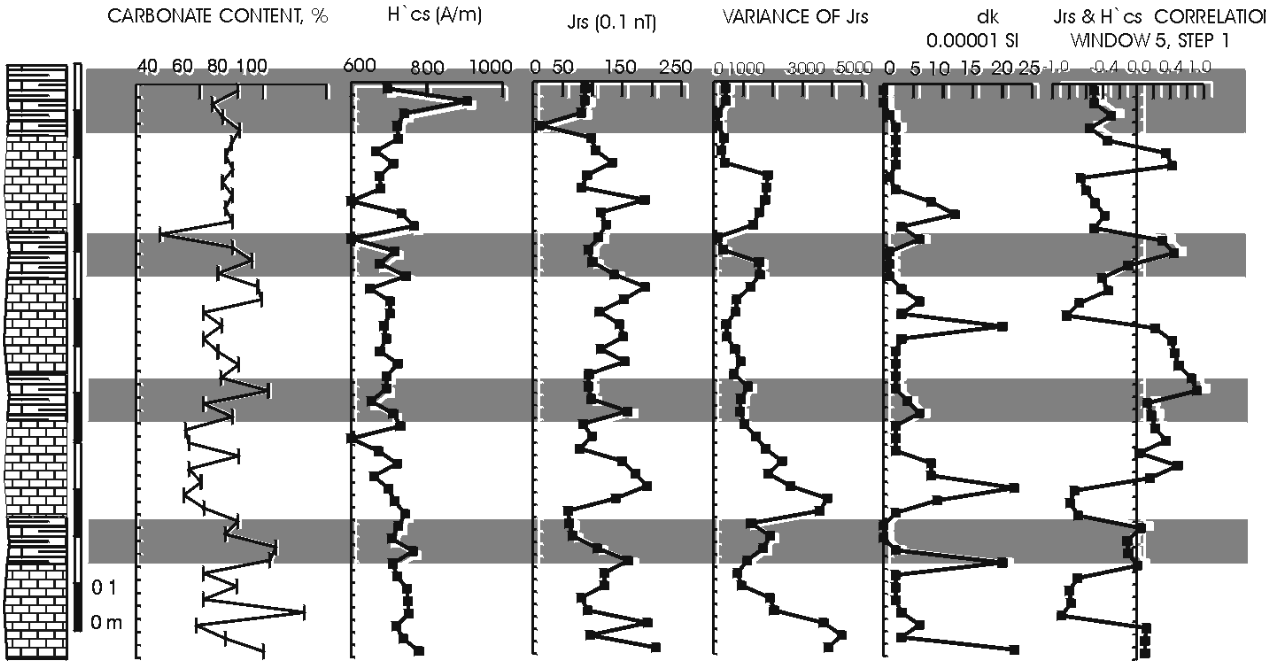


**Fig. 5.** Detailed distribution of carbonate content and petromagnetic parameters in Middle Cenomanian (petromagnetic complex No. 2) limestone-marl rhythms of Selbuhra section, SW Crimea.

## Stratigraphy

Lower Cenomanian rhythmically bedded marls contain *Puzosia planulata* (Sow.) and *Inoceramus crippsi* (Mantell). This stratigraphic interval is characterized by the Mantelliceras mantelli Zone; Inoceramus crippsi Subzone or Thalmaniella deckei Zone (section 1). Rare remnants of plants and insects are known from these deposits.

Most parts of the Middle Cenomanian rhythmically bedded marls and limestones (sections 1, 2) include the ammonites *Mesogaudryceras leptonema* (Sharpe), *M. rarecostatum* Balan, *Galycoceras(?)* sp., the bivalves *Inoceramus virgatus* Schlut. and belong to the Rotalipora cushmani Zone (sections 1–3, 5).

Four petromagnetic complexes (PC) were determined by complex analysis of petromagnetic parameters in the Middle Cenomanian of Selbuhra Mountain (Cushmani Zone, Fig. 4). A brief schematic description of them is given here (Table 1). It should be noted, that the small quantity of samples in the uppermost part and in the bottom part of the investigated section results in an absence of calculated parameters. **PC 1.** Marls usually contain pyrite concretions and ichnofossils *Phycosiphon*, *Chondrites*, indicating low content of oxygen in water and rare *Planolites*. Limestones are characterized by ichnocoenoses: *Planolites, Zoophycos, Thallassinoides* and *Teichichnus*. **PC 2.** Pyrite concretions and the ichnogenus *Chondrites* are absent. **PC 3.** Ichnocoenoses: *Zoophycos, Teichichnus* and rare *Planolites* are present. Deposits of **PC 4** contain rare *Teichichnus* and *Zoophycos*. At the top of the Middle Cenomanian a bentonite layer was observed. Rocks of third and fourth petromagnetic complexes include pyrite concretions.

The Upper Cenomanian in the studied sections is poor in macrofossils: rare parts of the brachiopod *Lingula belbekensis* Klik. in section 3 (limestone couplets) and bivalves (inoceramids) in section 4 (limestone-marl rhythms). Remnants of deep marine fish were found in the black shales (Mazarovich & Mileev 1989). Calycoceras naviculare Zone of the Upper Cenomanian in the studied area was proved by D.P. Naidin (Naidin et al. 1975).

**Table l:** Sizes and distribution of studied parameters in the determined petromagnetic complexes (PC), Middle Cenomanian of Selbuhra Mountain.

| PC | k | Jrs | H'cs | dk | Jrs-H'cs correlation | Variance of Jrs |
|---|---|---|---|---|---|---|
| 1 | 7.5–25 | high | medium | high | positive | maximal |
| 2 | Extremely Chaotic distribution | medium, oscillation | minimal, oscillation | Absence (lower part) and high (upper part) | oscillation | oscillated decrease |
| 3 | minimal | high | high | high | negative | increase |
| 4 | minimal | minimal | medium | minimal | positive | high |

Upper Cenomanian rocks of Selbuhra Mountain consist of 2 petromagnetic complexes. Graph of Jrs-H'cs variance can be divided into 2 parts: lower (oscillation) and upper (no oscillation). Clear rhythmicity and the presence of the bentonite couplet is typical for the lower complex (**PC 1**). Deposits of the upper complex (**PC 2**) lose rhythmicity near the Cenomanian-Turonian boundary (chaotic distribution of layers). The Upper Cenomanian rocks (Selbuhra section) are characterized by medium Jrs-H'cs variance and low correlation. H'cs varies from 600 to 700 A/m.

The petromagnetic section of Mender Mountain (Upper Cenomanian) can also be divided into 2 complexes. The lower complex (**PC 1**) is characterized by relatively high medium size of Jrs (27.5 nT), the upper complex (**PC 2**) by relatively low size of Jrs (medium—22.1 nT). This section

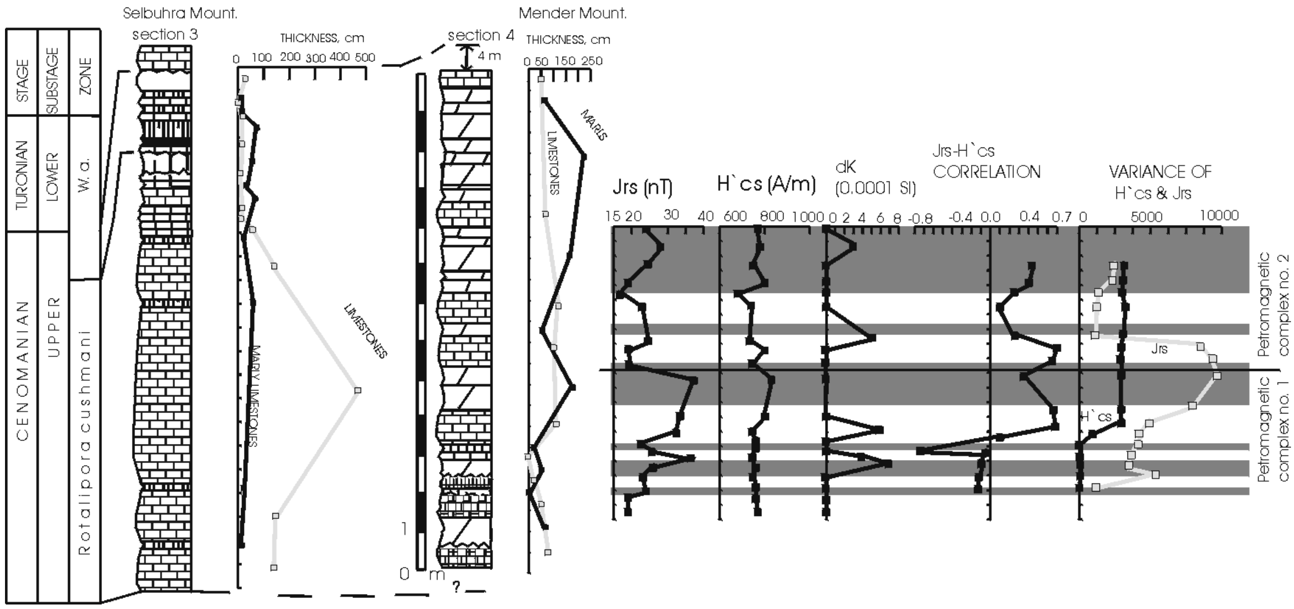


**Fig. 6.** Scheme of correlation, thickness distribution of Upper Cenomanian carbonate rocks (Selbuhra & Mender section) and distribution of petromagnetic paramaters (Mender section) of Bakhchisarai region, Crimea.

(Fig. 6) is characterized by absence of pyrite concretions and low sizes of dk.

## Description of rhytmicity types

In studied area rhythmicity can be divided into 5 types.

**First type**. Rhythms of marl-sandy marl; Lower Cenomanian (Mantelliceras mantelli Zone, Inoceramus crippsi Subzone), section 1 (Fig. 2). Boundaries between rhythm elements are not distinct. There are only small difference between composition of rhythm elements (Table 2). The rhythms in the Zong Shan section (Tibet) of the Upper Cenomanian (Rotalipora cushmani Zone), could be similar to this type (Lamocda & Wan 1996).

**Second type**. Rhythms of limestone-marl; Upper Cenomanian (Rotalipora cushmani, Whiteinella archeocretacea zones), section 4 (Fig. 6). Boundaries are distinct, bioturbation is absent, carbonate content decreases towards the top of the section (to the Cenomanian-Turonian boundary). Thickness of marls strongly varies and increases to the top of the section (the thickness of the limestone beds is nearly constant). Marls prevail in the section. The composition of rhythm elements is shown in the Table 3.

**Third type**. Rhythms of limestone-marly limestone, marl; Middle Cenomanian (Rotalipora cushmani Zone), sections 1, 2, 5 (Fig. 3). Boundaries are different: erosive (8); transitional, diffuse (6); usually distinct. The quantity of pyrite concretions and carbonate content increase, bioturbation decreases to the top of the section (Fig. 4). Few rhythms were profoundly investigated (Fig. 5). Elements of the rhythm show the difference in content of carbonate, clay, terrigenous minerals, bioclasts (Tables 4, 5). The planktonic/benthic foraminiferal ratio is different in the rhythm elements.

**Fourth type**. Rhythms of limestone-limestone (due to different carbonate content), Upper Cenomanian (Rotalipora cushmani Zone), section 3 (Fig. 8). Boundaries are not distinct, bioturbation is absent or rare, carbonate content increases towards the top of the section (to the Cenomanian-Turonian boundary). Thickness of rhythm elements strongly varies, limestones 1 dominate in the section. Their thickness increases towards the top of the section (the thickness of the limestones 2 is nearly constant). The composition of the rhythm elements (RE) is shown in the Table 6.

**Fifth type.** "Black shale" cyclicity: marly clay-marl rhythms with 6 horizons of limonite and pyrite concretions. Upper Cenomanian–Lower Turonian (Rotalipora cushmani, Whiteinella archeocretacea zones), Aksu-Dere Valley (section 6, Fig. 7). Fish remnants in marl couplets were found. This section was investigated by a group of authors, but the

**Table 2:** The comparison of rhythm elements (composition, texture etc.) of the Lower Cenomanian, Selbuhra section.

| | Marl | Sandy marl |
|---|---|---|
| Calcium carbonate, % | 65–71 | 60–70 |
| TOC, % | 0.05 | 0.05 |
| Colour | grey | dirty green, grey |
| Thickness, m | 0.4–0.1 | 0.2–0.4 |
| Bioturbation | medium | medium |

**Table 3:** The comparison of rhythm elements (composition, texture etc.) of the Upper Cenomanian, Mender section.

| | Limestone | Marl |
|---|---|---|
| Calcium carbonate, % | 81–70 | 80–65 |
| TOC, % | 0.1 | 0.29 |
| Colour | white | white |
| Thickness, m | 0.8–1.2 | 0.3–2.24 |
| Bioturbation | is absent or rare | is absent or rare |

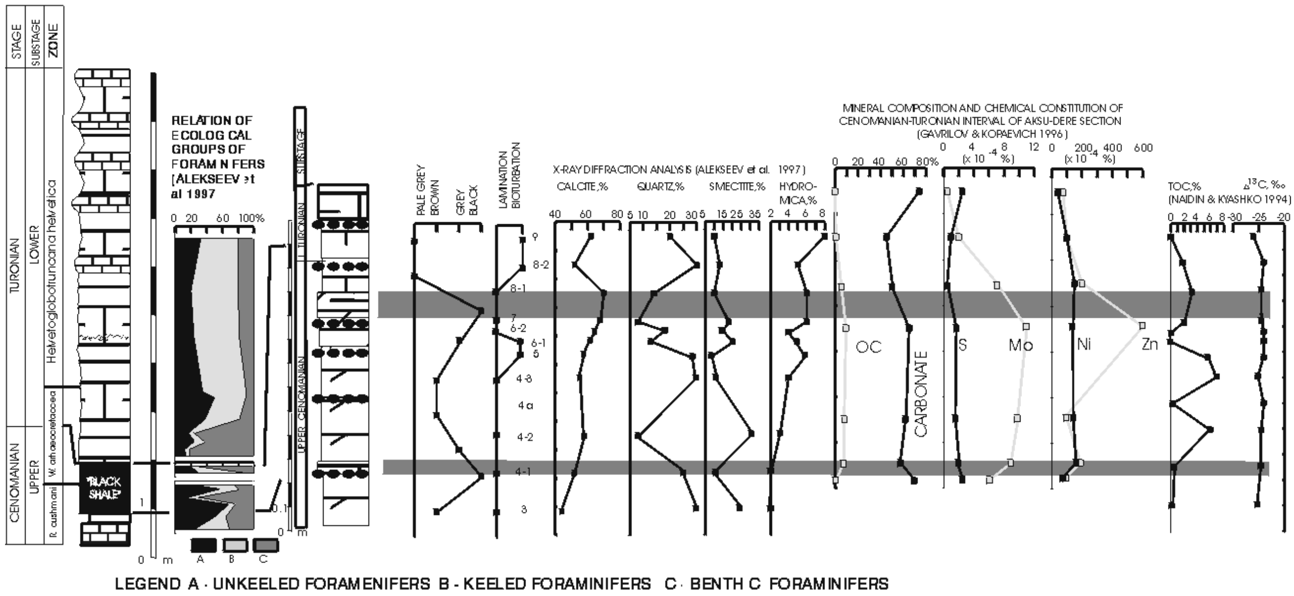


**Fig. 7.** Rhythmically bedded Upper Cenomanian (“Black Shale”) and Lower Turonian rocks of Aksu-Dere Valley, SW Crimea.

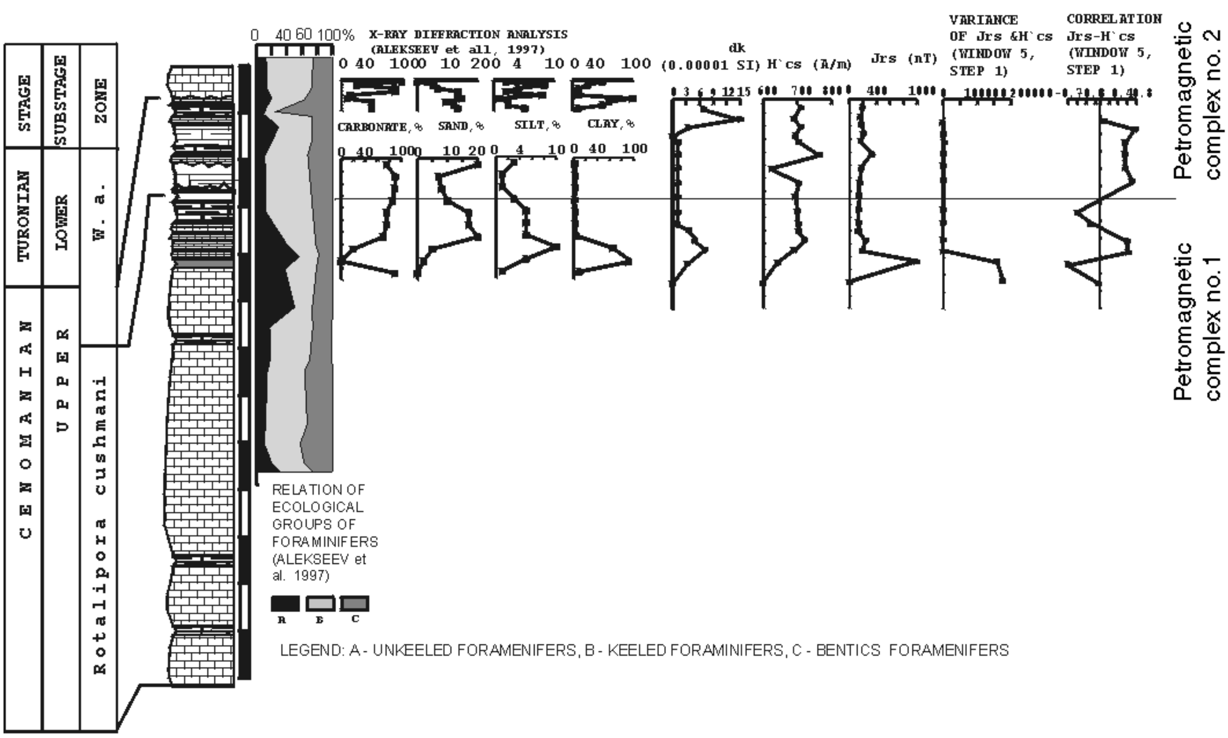


**Fig. 8.** Upper Cenomanian rocks of Selbuhra Mountain.

data of analyses, interpretation, field description is sometimes different (Table 7). Shale and adjacent layers can be divided into 6 rhythms (marked by 6 horizons of limonite and pyrite concretions). Each rhythm consists of a marly clay-marl alteration. Inside the "shale" two black marls were observed. The presence of 2 black couplets and 6 horizons indicates the maximal anaerobic conditions (no bioturbation). Other layers were formed in a dysaerobic regime. Data of S, Mo, Ni, Zn distribution (Gavrilov & Kopaevich 1996) did not show cyclic fluctuation.

**Table 4:** The mineral composition of rhythm elements according to X-ray diffraction data (PC 1, Middle Cenomanian, Selbuhra section).

| | Limestone | Marl |
|---|---|---|
| Calcite, % | 88.8 | 69.7 |
| Illite, % | 4.5 | 12.6 |
| Mixedlay, % | 0.7 | |
| Quartz, % | 5.3 | 8.4 |
| Rutile, % | 0.8 | |
| Chlorite, % | | 0.4 |
| Microcline, % | | 1.4 |
| Montmorillonite, % | | 7.5 |

**Table 5:** The comparison of rhythm elements (composition, texture etc.) of the PC 2, Middle Cenomanian, Selbuhra section.

| | Limestone | Marly limestone, marl |
|---|---|---|
| Carbonate, % | 95–70 | 85–47 |
| TOC, % | 0.08 | 0.44 |
| Colour | white | grey |
| Thickness, m | 0.08–1.3 | 0.1–0.6 |
| Foraminifera P/B,% | 5.5 | 5 |
| Carbon isotope 13,% (Frolov 1996) | 20–30 | 20–30 |
| Oxygen isotope 18,% (Frolov 1996) | –20 | –5 |
| Sea water temperature, degrees centigrade (Frolov 1996) | 23–25 | 14–15 |
| Ichnofossils & Bioclasts | > | < |

**Table 6:** The comparison of rhythm elements (composition, texture etc.) of the Upper Cenomanian, Selbuhra section.

| | Limestone 1 | Limestone 2 |
|---|---|---|
| Calcium carbonate, % | 95–75 | 94–70 |
| TOC, % | 0.06 | 0.17 |
| Colour | white | white |
| Thickness, m | 0.4–4.7 | 0.1–0.5 |
| Bioturbation | is absent or rare | is absent or rare |

**Table 7:** The comparison of rhythm elements (composition, texture etc.) of the Upper Cenomanian-Lower Turonian, Aksu-Dere section.

| | Marl | Marly clay |
|---|---|---|
| TOC, % (Gavrilov & Kopaevich 1996) | 0–9 | 0–9 |
| TOC, % (Naidin & Kyashko 1994) | 0–2 | 0–7 |
| Carbonate, % (Gavrilov & Kopaevich 1996) | 65–70 | 45–60 |
| Colour | grey, black | pale grey, brown |
| Texture | Bioturbation or lamination | L amination |
| Calcite, % (Alekseev et al. 1997) | 60–70 | 42–60 |
| Quartz, % (Alekseev et al. 1997) | 7–25 | 10–30 |
| Smectite, % (Alekseev et al. 1997) | 10–17 | 10–30 |
| Hydromica, % (Alekseev et al. 1997) | 0–6 | 3–8 |

## Discussion

There is a group of questions about the origin of rhythmically bedded Cenomanian carbonate rocks:

(1) Which models explain the origin of the rhythms in pelagic/hemipelagic carbonate rocks?

(2) What mechanisms are responsible for the occurrence of defined types of rhythmicity?

(3) Which paleogeographical models are suitable for the studied sections?

(4) Which parts of the basin are represented by studied sections?

(5) Which agent is responsible for diversity of rhythm types in the Late Cenomanian?

(6) Why does the succession lose rhythmicity near the Cenomanian-Turonian boundary?

(7) What is the frequency (time periodicity) of rhythms?

Different models are suggested to explain the origin of the rhythmically bedded pelagic/hemipelagic carbonate rocks (Fig. 9). They can be briefly described.

**Dilution cycles. Model 1** (Einsele 1985). Cyclic changes of moisture, terrestrial input due to climatic variations form rhythmicity in the carbonate sediments. During a dry climate mostly limestones are deposited. A wet climate is a time of marls, with dilution of the constant carbonate sedimentation by terrigenious material (clay), transported by rivers.

**Dilution cycles. Model 2** (Ruffel et al. 1996). This model is close to the first one. The difference is that in the first case cyclic climatic changes result in the cyclic changes in volume of run off, but here climatic fluctuations cause variations in the nature of weathering and in the composition of the terrigenious material constantly transported by rivers. The wet, (or) warm season is a time of marl sedimentation. Limestones occur during dry, (or) cold conditions.

**Dilution cycles. Model 3** (Morozov 1952). Sea level rise is a time of transgression (ingression) which causes washing out of accumulated terrestrial material from the shore districts into the basin. So, a relatively high terrigenious input takes place. Sea level fall is a time of regression and relatively low terrestrial input.

**Dilution cycles. Model 4** (Gavrilov & Kopaevich 1996). During sea level fall shore districts become a territory with swamps and deposition of organic rich sediments. Sea level rise causes transportation of sediments into the basin (deposition and partial dissolution, increase of bioproductivity), appearance of anaerobic conditions and occurrence of "black shales".

**Solution cycles. Model 5 (**Gabdullin & Baraboshkin 1997). Cyclic repetition of condensation and deposition result in appearance of rhythmic limestone-carbonate clay (marl) sections. The limestones always have an erosional contact with clays (marls). The limestones represent a sedimentation regime, condensation causes the appearance of carbonate clay, marl (result of limestone dissolution). Erosional surfaces occur due to a non-depositional regime and include soft- and hard-grounds. Condensation and sedimentation are proposed to be cyclic processes.

**Solution cycles. Model 6** (Einsele 1985). SLC causes variation of the critical carbonate solution depth. Periodically the solution volume of the constantly deposited carbonate changes.

**Solution cycles. Model 7** (Ricken 1994). Sea level change causes cyclic depth variation of the basin, which results in periodic occurrence of stratified waters with anoxic or nearly anoxic conditions and solution of the constantly deposited carbonates. Sea level up — marl, sea level down — limestone.

**Solution cycles. Model 8** (Savdra & Bottjer 1994). Climatic variations result in fluctuations of winds and water current direction, which cause changes in the content of oxygen dissolved in bottom waters. Because of new current directions and some specific bottom relief forms stagnate, stratified water masses can occur. Cyclic changes aerobic-dysaerobic-anaerobic conditions result in periodic solution of constantly deposited carbonates.

**Dilution and solution cycles. Model 9** (Hay 1996). Periodical volcanic input into a basin with mostly carbonate sedimentation causes cyclic appearance of bentonite couplets inside chalk or marl layers. Eruption affects in the occurrence of ash clouds and acid rain. Acid rain enriches the water of the basin with acids dissolving the carbonate.

**Cycles of bioproductivity, dilution, solution. Model 10** (Fischer & Arthur 1977). The whole history of the organic world can be divided into polytaxon and oligotaxon intervals (Fischer-Arthur cycles), which occur due to climatic variations, SLC.

**Solution cycles. Model 11** (Einsele 1985). Changes in the global carbon cycle result in variations of atmospheric chemistry and, hence, in climate. The carbon/oxygen relation depends on the volume of vegetation. A higher quantity of plants causes a lower content of carbon dioxide.

There is no precise data about the frequency and the time scale of the rhythms presented in the 11 models. It can be summarized that there are short period rhythms (1, 2) and long period rhythms (10, 11). The extent of the rhythmic bedding can be local (1-4, 8) and global (9-11).

Five types of rhythms were observed in the investigated region. We propose models 1-4, 7, 9, 10 to understand the origin of the studied rhythms.

The **first type** of rhythm can be interpreted as dilution cycles. Sandy marls rich in benthic fossils (mostly Inocéramides), different quantities of terrigenous material in the rhythm elements (relatively higher content then in other sections) show the relatively shallow marine conditions in the basin of sedimentation which was situated close to the land (remnants of plants and rare insects). The presence of forests with insects indicate a warm, wet climate. Diagenetic overprint is possible. We propose that these rhythms are classified as dilution cycles (model 1, Fig. 9).

**Second type**. Increase of Jrs is thought to be connected with increase of terrestrial input of magnetite. The type of input (absence of sulphides) is proven by the low sizes of magnetic susceptibility and variances of Jrs and H'cs, low size of Jrs-H'cs correlation. The absence of wide oscillations on the graph of the Jrs-H'cs correlation was interpreted as nearly constant dilution (model 2). Increasing thickness of marls rich in bivalves demonstrates cyclic changes in the carbonate bioproduction (model 10, Fig. 9). Models 2 and 10 are suitable for interpretation of the origin of the second type of rhythm.

Probably, the same type of rhythm is typical of the Middle Cenomanian part of the Castagne section, S. Italy (Claps & Masetti 1994).

**Third type**. The estimated sea water temperature (based on the isotope method) during the time when a limestone bed accumulated was about 23-25 $^{o}$C. Marls and marly limestones were formed in water with a temperature of 14-15 $^{o}$C (Frolov 1996). Marl couplets contain more terrestrial material, than limestone beds. This can be interpreted as evidence that a warm, dry climate periodically changed into a cold wet climate. However, the precise investigation and division of Middle Cenomanian rocks into 4 petromagnetic complexes shows a more complicated behaviour of the dilution agent.

Petromagnetic rhythmicity proves dilution cycles in the Middle Cenomanian section of Selbuhra. Particles of pyrite and pyrrothine are of allochthonous origin (DTMA data). This can be supported by low size of Keninberger's parameter (0.01-0.1). At the same time there is data about authigenic pyrite in the studied section. High positive Jrs-H'cs correlation can be interpreted as indicating the presence of two Fe-magnetic minerals. The presence of only one magnetic mineral in the rock is defined by diverse (negative) Jrs-H'cs correlation. A positive correlation with an essential increase of magnetic susceptibility proves the presence of two minerals: pyrite and pyrrhotine. Negative correlation with the absence of magnetic susceptibility increase indicates the presence of magnetite. The Middle Cenomanian was a time when terrestrial input (Table 8) included magnetite (type 1) or magnetite and sulphides (type 2). The oscillations (positive-negative) on the graph of Jrs-H'cs correlation (PC 2) are interpreted as dilution cycles. Petromagnetic complexes 1, 3 and 4 are characterized by constant dilution (absence of positive-negative oscillations).

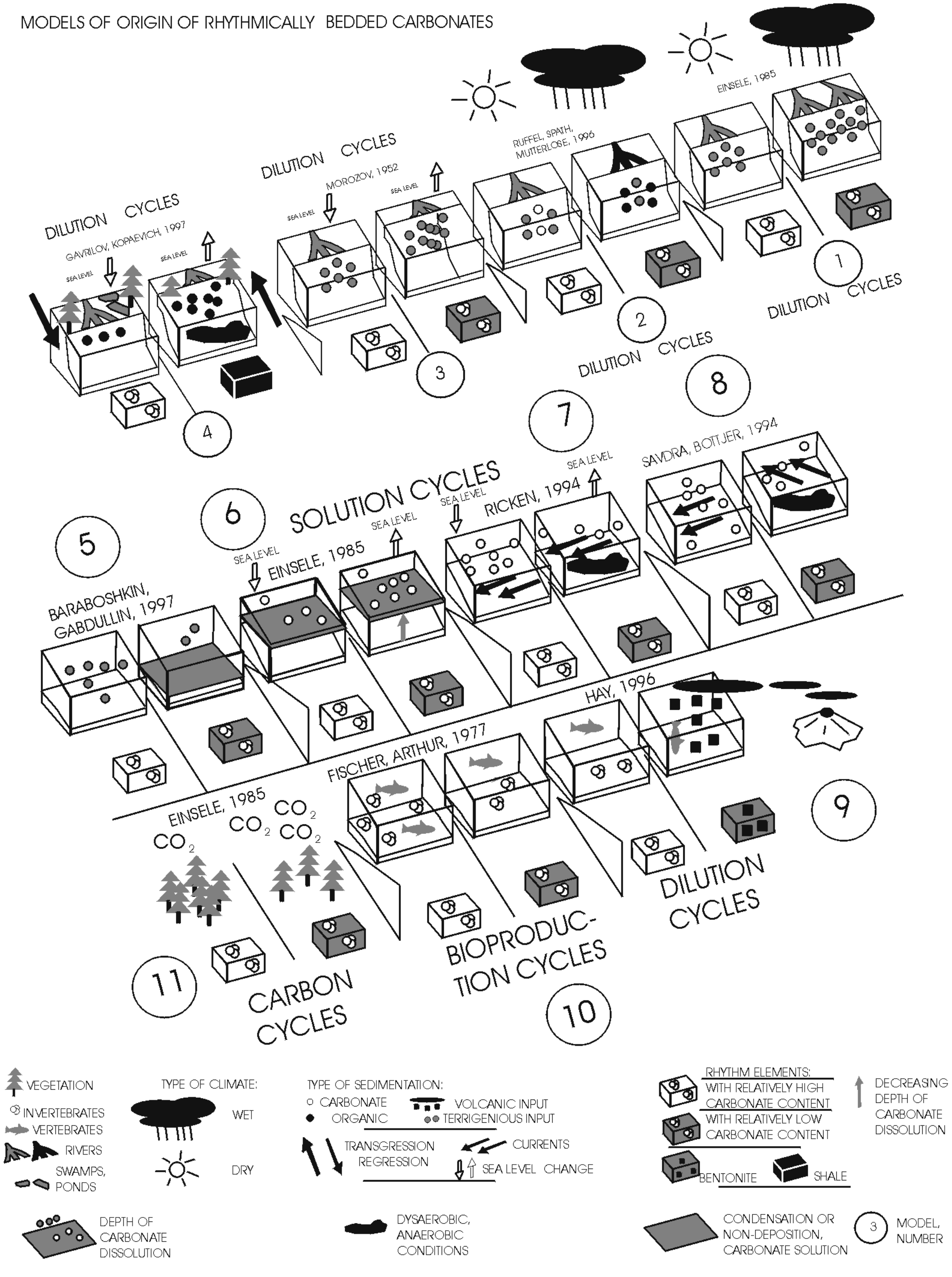


**Fig. 9.** Models of origin of rhythmically bedded carbonates.

**Table 8:** Distribution of authigenic and allogenic minerals in the determined petromagnetic complexes (PC) in Middle Cenomanian of Selbuhra Mountain.

| PC | Authigenic minerals | Allochthonous minerals | Type of input | Comments |
|---|---|---|---|---|
| 1 | | magnetite & sulphides | 2 | constant input |
| 2 | | magnetite & sulphides | 2 | oscillated input |
| 3 | pyrite | magnetite | 1 | constant input |
| 4 | pyrite | | | |

**PC 1** (lower part of the Middle Cenomanian in section 1) is connected with the second type of constant terrestrial input of different composition (Table 4). Model number 1 is suitable. At the same time solution cycles influenced the sedimentation system. Fluctuations in the oxygen content in the bottom waters are proven by different concentrations of organic carbon, pyrite concretions and the volume of bioturbated rocks in RE. Ichnofossils *Planolites, Zoophycos, Teichichnus, Chondrites, Thallassinoides, Phycosiphon* observed at the outcrop belong to different bathymetric zones and cannot coexist. Cyclic distribution of ichnocoenoses means variations not only in oxygen content but also sea level change (model 7). Models 1 and 7 are proposed.

**PC 2** is characterized by oscillating input of magnetite and sulphides (dilution cycles). Each subsequent volume of input was smaller then the previous one. This is proven by constant decrease of amplitude of oscillation on the graph of Jrs-H'cs correlation in the direction of the top of the section. We can conclude that the denudation area was periodically submerged and each successive sea level rise was relatively higher or the distance to the source constantly increased. It should be noted that many peaks of dk (up to $5\times10^{-6}$ SI) indicate the sulphide concentration and are not connected with the volume of input. Dilution cycles during sea level change are described by model 3.

**PC 3.** Terrestrial constant input of magnetite (type 1). No sulphides were transported from the land, but increase of dk can be interpreted as authigenic sulphide deposition caused by anaerobic–dysaerobic conditions during sea level rise. Erosive boundaries between rhythm elements were found. Constant dilution (model 2) and solution (model 7) took place.

**PC 4** is characterized by minimal size of dk and Jrs. It was a time, when terrestrial input decreased and the basin was deeper than during the time of accumulation of sediments of previous petromagnetic complexes. Erosive boundaries between RE and rare pyrite concretions prove solution cycles. At the top of the PC 4 (top of the Middle Cenomanian) a bentonite bed was observed. Sediments of this petromagnetic complex were accumulated in the conditions of volcanic dilution and solution. Model 9 is proposed.

**Fourth type.** The Upper Cenomanian limestones of Selbuhra Mountain (section 3) were divided into two parts. Increase of dk without increasing of Jrs can be connected with authigenic sulphides (pyrite) formed during dysaerobic conditions. Sediments were deposited with terrestrial input of magnetite (type 1).

**PC 1** (lower part of the Upper Cenomanian). Dilution cycles are determined by oscillation of the graph of Jrs-H'cs correlation and peaks on the graphs of composition of rocks determined by XRD analysis. Variations in the thickness of limestone 1 layers (1–4 m) are thought to be caused by bioproduction cycles. The nearly constant P/B relation in RE (Fig. 8) indicates no change of the sea level. The presence of one bentonite layer and absence of any solution traces in the section is unsufficient to support model 9. Proposed models: 1 and 10 (Fig. 9).

**PC 2** (upper part of the Upper Cenomanian). This unit is characterized by the constant dilution (model 2). Variations in P/B relation (Fig. 8) were interpreted as sea level change. Authigenic sulphides detected by petromagnetic data, rare bioturbation and presence of 3 erosional surfaces indicate solution regime (model 7). Proposed models: 2 and 7 (Fig. 9).

The relatively high medium size of Jrs (18.2 nT) in the Upper Cenomanian and relatively low medium size of Jrs (8.1 nT) in the Middle Cenomanian of Selbuhra section (previous type) can be interpreted as evidence of an increase in the volume of terrestrial material and a probable increase of tectonic activity in the basin of sedimentation with gradually increasing depth. In the Early Cenomanian a shallow basin existed (Fig. 1b) and marl/sandy marl rhythms (type 1) were formed in it. In the Middle Cenomanian (Fig. 1c) the basin became deeper and limestone-marl rhythms (type 3) were deposited. The Late Cenomanian (Fig. 1d) was characterized by the relatively deepest conditions and the appearance of limestone-limestone rhythms. Tectonic conditions changed at the begining of the second half of the Late Cenomanian from the relatively stable (lower complex) to relatively unstable (upper complex).

Types 3, 4 of the Middle and Upper Cenomanian rhythms (Crimea) could be similar to the Cenomanian of Scaglia Bianka Formation: couplets of carbonate rocks with similar thicknesses of rhythm elements (Schwarzacher 1994).

The **fifth type** of rhythmicity is thought to be connected with solution cycles (dysaerobic–anaerobic fluctuations defined by distribution of ichnofossils, rhythms inside "black shale", 6 horizons of limonite and pyrite, mineral composition of rocks, presence or absence of foraminifers) and possible dilution cycles (cyclic distribution of quartz grains). Earlier, model 4 (Fig. 9) was proposed for this section (Gavrilov & Kopaevich 1997). Model 7 (solution cycles) is also suitable.

## Evolution of the Cenomanian sedimentary system

The Lower Cenomanian is presented by shallow deposits rich in macrofossil invertebrates and marl-sandy marl succession (Selbuhra section, Figs. 1b, 2). The estimated depth of the basin containing remnants of plants and insects was about 40 m. Transgression, started in the Early Cenomanian affected in constant deepening of the basin and Middle Cenomanian rocks are poor in macrofossils and are presented by rhythmically bedded limestones and marls (Selbuhra and Kacha sections, Figs. 1c, 2). Deeper conditions are typical for Late Cenomanian (Fig. 1d).

The Upper Cenomanian rocks contained 3 types of rhythmicity: marly clay-marl rhythms (Aksu-Dere Valley), limestone-marl rhythms (Mender Mountain), limestone rhythms (Selbuhra Mountain). The end of the Cenomanian in the studied region (Aksu-Dere section) is characterized by an oceanic anoxic event (analogue of "the Bonarelli level"). At the same time in the Selbuhra section (Upper Cenomanian) the thickness of RE increase up to the first meters (instead of the first decimeters in the Middle Cenomanian), then rhythmicity disappears or changes into chaotic distribution of layers (2 meters beyond the Cenomanian-Turonian boundary). Petromagnetic interpretation of data from the Upper Cenomanian sections could support the idea of an increase of tectonic activity towards the end of the Cenomanian and a profound change in the hydrodynamics and depth of the basin. The Selbuhra section loses its rhythmicity, the Aksu-Dere section contains "black shales", the Selbuhra section (before the arrhythmic interval of the succession) and Mender sections consist of thick rhythms (1–4.5 m). A.S. Gale found (pers. communication) syngenetic microfaults in the rocks of the Selbuhra section a few meters beyond the Cenomanian-Turonian boundary. We suggest a tectonic factor is responsible for the disappearance of rhythmicity in the Late Cenomanian. Data derived in this project is insufficient to make more concrete conclusions about the nature of the disappearance of rhythmicity at the end of the Cenomanian.

Bentonitic couplets in the studied region are found in the Upper Cenomanian and at the boundary between the Middle and Upper Cenomanian (Selbuhra sections). So, weak volcanic influence upon sedimentation was possible.

The depth of the basin according to ichnofossils data, fish data obtained by A.S. Alekseev (Mazarovich & Mileev 1989) varies in the interval of the first hundred meters — shelf to the shelf edge. It is obvious, that the limestone-marl rhythms of Mender section rich in macrofossils were deposited in a shallower part of the basin, than the limestone rhythms of Selbuhra Mountain. From this point of view the Upper Cenomanian of the Mender section is close to the Middle Cenomanian of the Selbuhra section. The relatively high size of Jrs (up to 40 nT) in the Upper Cenomanian of the Mender section (Fig. 6) and relatively low size of Jrs (20–30 nT) in the Upper Cenomanian of the Selbuhra section (Fig. 8) can be defined as a relatively high input in the first case and relatively low — in the second, or the rocks of the Selbuhra section were deposited in deeper water than the rocks of the Mender section. The rocks of the Aksu-Dere section (Fig. 7) presented by "black shale" rich in remnants of deep marine (sea level rise), were formed in the part of basin with stratified water masses under an anaerobic regime. It was a time of deposition of black marls. Periodically conditions became dysaerobic and marly clays were deposited.

This described rhythmicity could be the result of the global, orbital forced cyclic processes — Milankovitch cycles.

The determination of time periodicity of rhythmicity seems problematic. Firstly, part of the Cenomanian is not exposed (most of the Lower Cenomanian and base of the Middle Cenomanian). Secondly, the Cenomanian of Crimea contains many erosive boundaries at the base, at the top and inside the succession. A.S. Gale considers (pers. communication) that the origin of limestone-marl rhytms of the Middle Cenomanian (Selbuhra Mountain, type 3) could be connected with precession cycles.

## Conclusions

(1) There are 11 models for the origin of carbonate rhythms, 7 models are proposed by authors for the studied sections. Models number 1, 2 and 7 were used three times.

(2, 3) Dilution cycles and possible diagenetic overprint are responsible for the occurrence of marl-sandy marl rhythms of the first type (Lower Cenomanian, Mantelliceras mantelli Zone, Inoceramus crippsi Subzone) in the Selbuhra section (model 1). Constant dilution, bioproduction cycles caused the appearance of marl-limestone rhythms of the second type (Upper Cenomanian, Rotalipora cushmani Zone) in the Mender section (models 2, 10). Sections with limestone-marly limestone or marl rhythms of the third type (Middle Cenomanian Rotalipora cushmani Zone) on the slope of Selbuhra Mountain were divided into four petromagnetic complexes. PC 1 — cycles of dilution and solution, models 1 and 7. PC 2 — constant dilution, model 3. PC 3 — constant dilution, solution cycles, models 2 and 7. PC 4 — volcanic dilution and solution cycles, model 9. Rhythmic section of the fourth type: limestone-limestone cycles from the Upper Cenomanian (Rotalipora cushmani Zone) of Selbuhra Mountain was subdivided into two petromagnetic complexes. PC 1 — cycles of dilution and bioproduction, models 1 and 10. PC 2 — constant dilution and solution cycles, models 2, 7. "Black shale" cyclicity: marly clay-marl rhythms with 6 horizons of limonite and pyrite concretions. Upper Cenomanian-Lower Turonian (Rotalipora cushmani, Whiteinella archeocretacea zones) marly clay-marl rhythms from the Aksu-Dere section occurred due to solution and dilution cycles, models 4 and 7.

(4) The investigated Upper Cenomanian sections represent different parts of the same basin (distance between outcrops is about 3–7 km). The shallowest conditions were established in the Mender section (limestone-marl rhythms with complex of benthic fossils). Shallow conditions are proven for the Selbuhra section (limestone-limestone rhythms with absence of macrofossils) and depression with anaerobic–dysaerobic regime or the relatively deeper part of the basin — Aksu-Dere section (marl-marly clay rhythms with abundant fish remnants).

(5) The types of rhythms can be classified on the basis of their lithology and paleogeographical position. Shallow marine types: 1 — marl-sandy marl (Early Cenomanian); 2 — marl-limestone (Late Cenomanian). Deep marine types: 3 — marl, marly limestone-limestone (Middle Cenomanian); 4 — limestone-limestone (Late Cenomanian); 5 — marl-marly clay rhythms in black shales (Late Cenomanian). Diversity of rhythm types in the Late Cenomanian (Mender, Selbuhra, Aksu-Dere sections) is connected with sedimentation of carbonates in different parts of the basin.

(6) A tectonic agent is responsible for the disappearance of rhythmicity near the Cenomanian-Turonian boundary in the Selbuhra section. To understand the nature and the driving

force of the tectonic factor more precise investigation must be done.

(7) The nature of Middle Cenomanian limestone-marl rhythms could be connected with precession cycles. It seems problematic to determine the time periodicity of the investigated rhythms because of the presence of erosive surfaces (gaps) in the succession, inadequate outcrops and the unexposed lower part of the Cenomanian section.

**Acknowledgments:** We greatly appreciated the assistance of Alexandr Widrik in taking samples and for help in the lab. We thank Helmut Weissert for the help and advises. This work was done with the support of RBS (RFFI, No. 96-05-65443, 98-05-64196).

## References

Alekseev A., Vengertsev V., Kopaevich L. & Kuzmicheva T., 1997: Lithology and micropaleontology of Cenomanian-Turonian boundary interval in SW Crimea. *Essay on the geology of the Crimea/ Transactions of the A.A. Bogdanov Crimean geological scientific-educational center*, Moscow, MSU, *Geol. Fac. Publ.,* 1, 54–73 (in Russian).

Claps M. & Masetti D., 1994: Milankovitch periodicities recorded in Cretaceous deep sea sequences from the Southern Alps. *Orbital forcing and the Milankovitch Theory, SPIAS*, 99–107.

Dolitskaya I., 1972: Particularity of foraminiferal distribution in Upper Cretaceous deposits of the Mountain Crimea. *News Sov. Acad. Sci., Geol.*, 3 (in Russian).

Einsele G., 1985: General data about nature, occurrence conditions and determination of cyclic deposits (periodities). In: Einsele G. & Zeilaher A. (Eds.): *Cyclic and event sedimentation*. *Mir*, Moscow, 11–15 (in Russian).

Fischer A. & Arthur M., 1977: Secular variations in the pelagic realm. In: Cook H. & Enos P. (Eds.): Deep-water carbonate environments. *Spec. Publ. Soc. Econ. Paleontologists Mineralogists*, 25, 19–50.

Frolov V., 1996: Lithology. *MSU Press*, Moscow, 3, 117–146 (in Russian).

Gabdullin R., 1997: Models of origin of rhythmicity in carbonate rocks. *Abstr. jub. sess. Russ. Acad. Sci., 28 February*, Moscow, 103–104 (in Russian).

Gabdullin R., 1997: The origin of rhytmically bedding in Middle Cenomanian carbonate rocks in the Bakhchisarai Region (SW Crimea). *Miner. slovaca*, 29, 269–271.

Gabdullin R. & Baraboshkin E., 1997: Rhythmicity in higly condensed sediments: sedimentary model of the Barremian “Cephalopod Limestones”of SW Crimea. *Abstr. 18-th IAS Reg. Eur. Meet. Sedimentol., Heidelberg, September 2–4,* 136.

Gavrilov J. & Kopaevich L., 1996: About geochemical, biochemical and biotic evidence of eustatic fluctuations. Stratigraphy. *Geol. Correlation*, 4, 4, 3–14 (in Russian).

Hay W.W., 1996. Tectonics and climate *Geol. Rdsch.,* 85, 409–437.

Mazarovich O. & Mileev V., 1989: Geological composition of the Kacha uplifting of the Mountain Crimea. *Mesozoic stratigraphy*. *MSU Press,* Moscow, 123–135 (in Russian).

Morozov N., 1952: About rhythmicity of sedimentation in Cretaceous in the region of Dono-Medveditskih dislocations. *Rep. Sov. Acad. Sci.*, LXXXVII, 2 (in Russian).

Naidin D. & Kyashko S., 1994: Characteristic of Cenomanian-Turonian boundary interval of Mountain Crimea. Part 1. Lithological composition, content of organic carbon and some elements. *Bull. Soc. Natur. Moscou*, 69, 1, 28–42 (in Russian).

Naidin D. & Maslakova N., 1958: About Cenomanian deposits of the Mountain Crimea. *USSR Acad. Sci. News, Geol.,* Moscow, 3, 108–110 (in Russian).

Naidin D., Vanchurov I. & Alekseev A., 1975: Using mathematical statistics methods in studding rostrums of the Cenomanian belemnites. *Bull. Soc. Natur. Moscou*, 50, 4, 81–94 (in Russian).

Lamocda M. & Wan X., 1996: The response of foraminifera to oceanic environmental changes during the Cenomanian-Turonian transition of Gamba Zong Shan section, Southern Tibet. *Cretaceous stratigraphy, paleobiology and paleogeography. Abstr. Jost Wiedmann symp., Tübingen, Germany, 7–10 March 1996*, 94–100.

Ricken W., 1994: Rhythmic sedimentation related to third-order sea-level variations. Upper Cretaceous, Western Interior Basin. *Orbital forcing and the Milankovitch Theory, SPIAS*, 167–193.

Ruffell A. & Spaeth C., 1996: Sedimentary and biogenetic cycles in the Early Cretaceous of NW Europe. In: Cretaceous stratigraphy, paleobiology and paleogeography. *Abstr. Jost Wiedmann symp., Tübingen, Germany, 7–10 March 1996*, 163–165.

Savdra C. & Bottjer D., 1994: Ichnofossils and ichnofabrics in rhythmically bedded pelagic/hemi-pelagic carbonates: recognition and evaluation of benthic redox and score cycles. *Orbital forcing and the Milankovitch Theory*, *SPIAS*, 195–210.

Schwarzacher W., 1994: Cyclostratigraphy of the Cenomanian in the Gubbio district, Italy: a field study. *Orbital forcing and the Milankovitch Theory*, *SPIAS*, 87–97.